MEMS Fourier Transform Spectrometer

Huseyin R. Seren,[1,2] N. Pelin Ayerden,[1], Sven Holmstrom[1], and Hakan Urey[1]

[1]Koç University, Electrical Engineering and Optical Microsystems Laboratory, Sariyer, Istanbul-TURKEY, nayerden@ku.edu.tr, sholmstrom@ku.edu.tr, hurey@ku.edu.tr

[2]Boston University, Mechanical Engineering 15 St Mary's Street Brookline, MA 02446-8200, hseren@bu.edu

Abstract

A comb actuated lamellar grating interferometer based MEMS Fourier Transform Infrared (FTIR) Spectrometer device is designed, fabricated and characterized. The device operates at out-of-plane resonant mode which will allow ultra miniaturized, sensitive, robust, and fast spectrometers. As a novel approach pantograph type springs are used in the mechanical design to achieve high deflections. The dynamic deformation on the gratings is minimized using additional suspension springs. Optical simulations are conducted to extensively analyze the device performance in terms of spectral resolution and signal-to-bias ratio (SBR). In the light of simulations and experiments, the grating geometry is optimized for the region of wavelengths of interest (2.5-16 µm). Comb structures are designed and placed around pantograph springs for low voltage operation. The fabrication process is developed based on CMOS compatible bulk micromachining of a silicon-on-insulator wafer. A maximum peak to peak mechanical deflection of 478 µm is acquired with 50 V p-p input voltage in ambient pressure.

1. Introduction

Principles of Fourier transform spectroscopy are known for decades and there are many commercial products. It is a widely used method for color measurement, quality and process control, gas detection and chemical analysis. FTIR have several advantages over other spectroscopy methods such as high signal to noise ratio, high throughput, compact form-factor and low cost. However, they are all delicate instruments suitable for lab use in a controlled and vibration-free environment. One of the most common interferometer configurations is the Michelson interferometer that contains a reference mirror, a movable mirror and a beam splitter. With the developments in microfabrication and micro-electro-mechanical systems (MEMS) technology, it is possible to fabricate dynamic diffraction based interferometers, also called lamellar grating interferometer (LGI), that essentially eliminates the reference mirror, thereby the long mechanical path between the reference and moving mirrors, and eliminates the need for beam splitter and dispersion compensation plate. These are all important and unique advantages offered by LGI as compared to traditional Michelson interferometers. In this paper a MEMS out-of-plane resonant actuator carrying a lamellar grating is designed, fabricated and characterized. To achieve very high deflections while keeping dynamic deformation at low levels, much attention has been paid to the design of the pantograph inspired hinges. The present optical design (Section 2) is largely based on the work previously done by our group in [1]. Mechanical design that is further developed compared to our previous work [4, 5] is explained in section 3, followed by characterization results in section 4. In section 5 early intereferometer results from a table mounted setup with the LGI device as the critical component is discussed.

2. Optical Simulation Results

Optical design of LGI device has many aspects that need to be carefully tailored. For intensive analysis we implemented scalar diffraction theory [2] using MATLAB (Fig. 1.a and Fig.1.b). We defined grating fingers as optical amplitude functions and computed the propagated beam passing through the fingers using our code. We found the intensity collected on the photodetector (or at the far field). The procedure is repeated at sample positions of moving grating and an interferogram is generated. The spectrum is computed by simply taking the Fourier Transform of the computed interferogram. For more accurate results, we simulated the diverging light source composed of superposed discrete plane waves at sample angles. Resulting spectrum contains valuable information about the optical design performance such as measurement resolution or signal strength [1]. We defined the maximum width of the grating as 5 mm and the maximum traveled distance of the moving grating set as 500 µm. The maximum source divergence is accepted as 2.5 degrees. In order to find the optimum grating period we repeated the simulation for various period lengths and for the interval of wavelength of interest (2.5-16 µm). Two figures of merits are defined which are the spectral resolution and the signal-to-bias ratio (SBR). The spectral resolution is found as the width between first zero

978-1-4244-6051-9/11/$26.00 ©2011 IEEE

crossings of the fitted Sinc function at the expected spectral frequency. SBR is defined as the ratio of the energies of the expected spectral frequency to the DC. The resulting resolution and SBR maps are given in Fig. 1.c.

According to Fig. 1.c the device performance becomes worse as the wavelength to grating period ratio increases. This effect is seen due to Talbot phenomenon which arises from the rapid diffraction of the light. If the reversed Talbot image distance coincides with the distance between the grating sets, most of the energy can escape through the gaps between the grating fingers degrading the interferogram, thus the measurement resolution and SBR. This critical distance is given by Eq. 1 for λ being the wavelength.

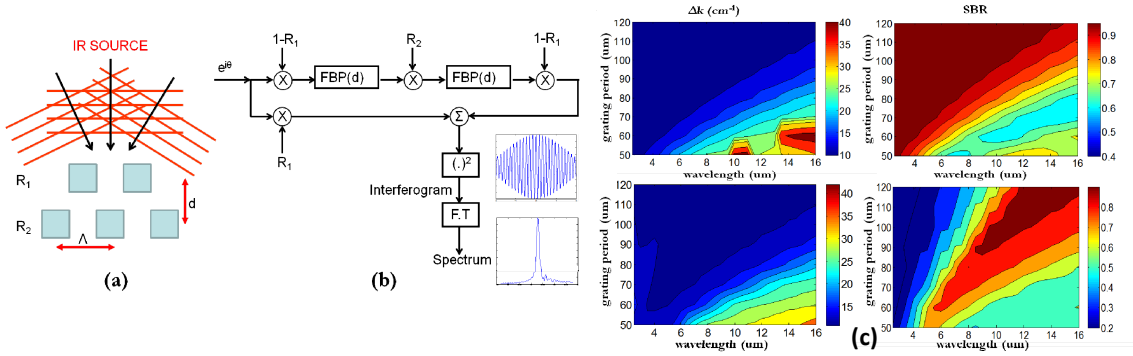

Figure 1: (a) Exemplary simulation layout (b) The simulation algorithm block diagram ($R_{1,2}$: Grating reflection functions, Λ: Grating period, d: distance between grating sets, FBP: Fresnel beam propagation function, FT: Fourier Transform) (c) Spectral resolution (Δk) and SBR maps for 0^0 divergence (upper) and 2.5^0 divergence (lower)

$$z_{talbot} = \frac{\Lambda^2}{\lambda} \tag{1}$$

The effect of beam divergence becomes apparent at the SBR map. At low wavelengths higher diffraction orders mix with the broadened 0th order due divergence. 180^0 phase difference between the 0th and higher orders increases the intensity of the collected light while decreasing the effect of the interference causing lower SBRs. In the light of our simulations, the grating period can be picked according to the needed resolution and detector properties. The gap size between the fingers and metalized grating reflectivity should also be noted for the optical performance maximization.

3. Device Design

To achieve the stroke needed for the LGI pantograph type of suspensions, originally introduced by Fraunhofer IPMS [3], are used. Pantograph suspensions have a highly efficient torsional motion conversion mechanism (Fig. 2). ANSYS finite element modeling software was used to model the mechanical structure. One of the main tasks during modeling is to make sure the desired operational out-of-plane mode is the first mode and in addition is well isolated from higher modes to avoid parasitic distortions. The springs are designed to afford a maximum motion of 500 µm out-of- plane deflection of the grating. Dual springs are used at each connection point to increase the operation survivability at large strokes. The largest expected stress on the springs is 1.1 GPa according to the simulation.

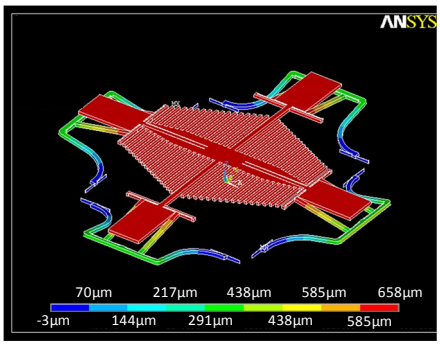

Figure 2: The first mode, deflection, of the device model. Bending takes place in the pantograph springs.

The device is fabricated with a standard four mask silicon-on-insulator process where the mechanically active part is formed by deep reactive ion etching from the device layer. 60 nm aluminum is deposited on top of the grating fingers. The thickness is selected as 75 µm thick to reduce the dynamic deformation. However, the most crucial step towards reducing the deformation was adding decoupling suspensions at the joints of pantographs. When the pantographs are directly connected to the body, the middle portion of the structure tends to bow and creates high deformations in the order of a couple of micrometers. These long and flexible suspensions on the four sides transfer the motion directly to the center of the grating structure and absorb most of the deformation on themselves. The joint positions of these suspensions were optimized and the grating body was tailored according to the deformation contour lines which gave it its present shape where simulated peak to peak deformation on the grating fingers is around 230 nm. For the electrostatic actuation eight separate comb-finger sets with 5 µm fingers are placed close to the hinges. As has been shown in several earlier publications there is no need for a vertical off-set for resonant actuation [6, 7]. Unavoidable fabrication aberrations will, when actuated at resonance, always be enough to start the vibration. Because of the parametric nature of the device the maximum deflection will be found when actuated at double the mechanical resonance frequency for the first mode.

4. Mechanical Characterization

Mechanical characterization of LGI devices with 130 µm pitch size is done using a laser Doppler vibrometer (LDV). Devices are excited with a square wave of 50% duty cycle with half of its p-p amplitude given as offset. Only comb fingers are used for electrostatic actuation and a maximum p-p deflection of 478 µm is obtained with 50 V p-p input voltage at an excitation frequency of 653.9 Hz in ambient pressure. The frequency response of this device is illustrated in Fig. 3. The vibration is sinusoidal and at half the excitation frequency. Voltage response shows linear behavior and due to nonlinear forcing function, minimum start voltage of the scanner is about 25V. Deflection further increases when grating fingers are used for actuation in addition to the comb fingers.

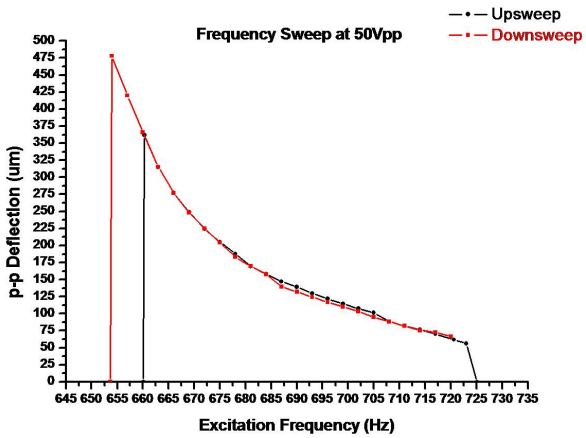

Figure 3: Frequency sweep at 50V_{pp} input voltage

5. Optical Characterization

In the optical setup illustrated in Fig. 4.a, an HeNe red laser with 632.8 nm wavelength and 0.8 mm beam diameter is directed at a beam expander to increase the laser beam size to about 5 mm. After the beam is expanded, it goes through an aperture to fix its size. Then, it passes through a beam splitter at 45° angle. After the beam is reflected from the device, it goes through the beam splitter again and gets imaged with a 300 mm focal length lens onto the detector. The focal length is chosen such that the diffraction orders are sufficiently separated so that the photodetector can detect only the 0th order. The aperture before the photodetector is used for blocking orders other than the 0th order. The signal that is detected by photodetector, interferogram, is recorded by an oscilloscope. The output of photodetector is composed of fringes with varying fringe frequency due to the sinusoidal speed variation of the device. Lastly, the interferogram is resampled in MATLAB such that the sinusoidals in it are equidistant and then its Fourier transform is calculated, which gives the spectrum. Fig. 4.b shows more details of the interferogram signal recorded at the photodetector.

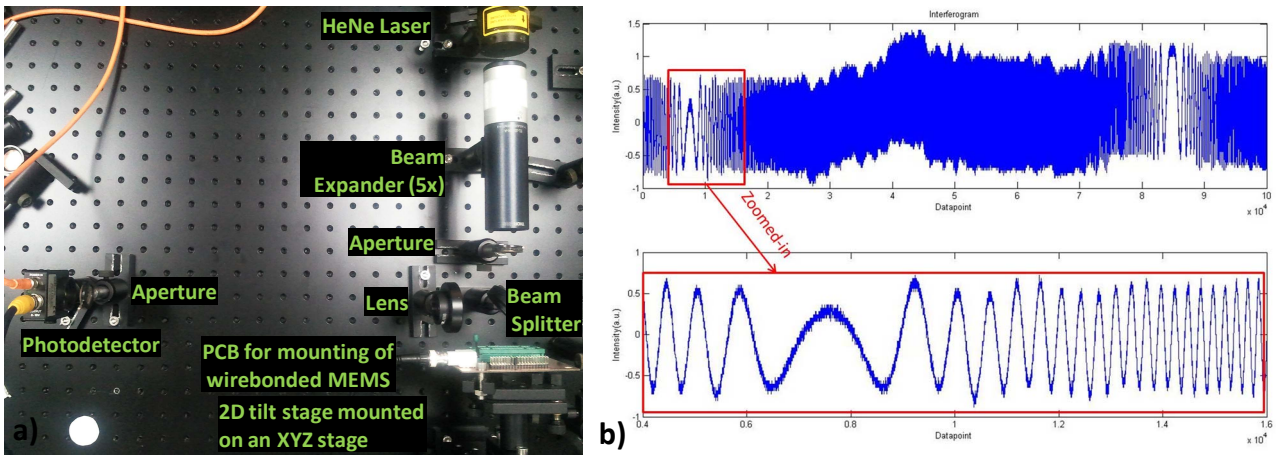

Figure 4: (a) Optical setup (b) Interferogram of device I. The device is excited at 647.7 Hz with 30V_{pp} input voltage. p-p deflection is 230 um.

5. Conclusion

FTIR spectrometer with out-of-plane resonant mode is implemented and characterized. Maximum peak-to-peak deflection of 478 µm is obtained with 50 V p-p input voltage at an excitation frequency of 653.9 Hz in ambient pressure. Early optical results are presented. Good interferogram data using the whole grating area is obtained due to static and dynamic flatness. Future work will be centered on calculating the spectrum using laser and blackbody IR light sources. Ultimately, whole system design will be completed with IR source and detector towards the project goal of achieving a resolution of 10 cm^{-1} in the infrared region.

6. Acknowledgments

This project is sponsored by MEMFIS project, which is supported by EC FP7 program grant no: 224151. The authors would like to thank all MEMFIS partners especially Fraunhofer IPMS, Bruker Optics and particularly Stephan Luettjohann for their contributions. Also, we would like to thank EPFL-CMI staff for their help with microfabrication.

7. References

1. O. Ferhanoglu, H. R. Seren, S. Lüttjohann, H. Urey, “Lamellar grating optimization for miniaturized Fourier transform spectrometers”, *Optics Express*, Vol. 17, Issue 23, pp. 21289-21301, 2009.

2. J. W . Goodman, Introduction to Fourier Optics, Roberts & Company Publishers, 2005.

3. T. Sandner, A. Kenda, C. Drabe, H. Schenk, W. Scherf, “Miniaturized FTIR-spectrometer based on optical MEMS translatory actuator”, *Proc. of SPIE*, Vol. 6466, 646602, 2007.

4. Caglar Ataman, Hakan Urey, Alexander Wolter, “MEMS-based Fourier Transform Spectrometer”, *J. Micromechanics and Microengineering*, Vol.: 16, Pages: 2516-2523, 2006.

5. H. R. Seren, N. P. Ayerden, J. Sharma, S. T. Holmström, T. Sandner, T. Grasshoff, H. Schenk, H. Urey, “Lamellar grating based Fourier transform spectrometer”, *IEEE Optical MEMS and Nanophotonics*, Sapporo, Japan, August 2010.

6. C. Ataman, H. Urey, “Modeling and characterization of comb-actuated resonant microscanners,” *Journal of Micromechanics and Microengineering*, vol. 16, pp. 9-16, 2006.

7. K. L. Turner, S. A. Miller, P. G. Hartwell, N. C. MacDonald, S. H. Strogatz and S. G. Adams, “Five parametric resonances in a microelectromechanical system,” *Nature*, vol. 396, pp. 149-152, Nov 1998.